

First-principles study of point defects in LiGaO₂

Adisak Boonchun,^{1,2} Klichchupong Dabsamut,^{1,2} and Walter R. L. Lambrecht^{3, a)}

¹⁾*Department of Physics, Faculty of Science, Kasetsart University, Bangkok 10900 Thailand*

²⁾*Thailand Center of Excellence in Physics, Commission on the Higher Education, Bangkok 10400, Thailand*

³⁾*Department of Physics, Case Western Reserve University, 10900 Euclid Avenue, Cleveland, Ohio 44106-7079, USA*

The native point defects are studied in LiGaO₂ using hybrid functional calculations. We find that the relative energy of formation of the cation vacancies and the cation antisite defects depends strongly on the chemical potential conditions. The lowest energy defect is found to be the Ga_{Li}²⁺ donor. It is compensated mostly by V_{Li}⁻¹ and in part by Li_{Ga}⁻² in the more Li-rich conditions. The equilibrium carrier concentrations are found to be negligible because the Fermi level is pinned deep in the gap and this is consistent with insulating behavior in pure LiGaO₂. The V_{Ga} has high energy under all reasonable conditions. Both the Ga_{Li} and the V_O are found to be negative U centers with deep $2 + /0$ transition levels.

I. INTRODUCTION

Recently, there has been an interest in ultra-wide-band-gap semiconductors such as β -Ga₂O₃ because of their potential in pushing high-power transitions to the next level of performance.^{1,2} An important figure of merit for such applications is the breakdown field and the latter is directly correlated with the band gap. Here we draw attention to an even higher band gap material, LiGaO₂. LiGaO₂ has a wurtzite-derived crystal structure^{3,4} and band gap of ~ 5.3 - 5.6 eV (at room temperature) based on optical absorption⁵⁻⁸ but potentially even as large as 6.25 eV (at $T = 0$) based on quasi-particle self-consistent (QS) GW calculations,⁹ with G the one-particle Green's function and W the screened Coulomb potential. It can be thought of as a I-III-VI₂ ternary analog of wurtzite ZnO, in which each group II Zn atom is replaced by either a group-I Li or a group III-Ga in a specific ordered pattern with the $Pbn2_1$ spacegroup. In this structure the octetrule is satisfied because each O is surrounded tetrahedrally by two Li and two Ga. The prototype for this crystal structure is β -NaFeO₂. LiGaO₂ can be grown in bulk form by the Czochralsky method³ and because of its good lattice match has been explored as a substrate for GaN. It can also be grown by epitaxial methods on ZnO and vice versa. Mixed ZnO-LiGaO₂ alloys have been reported.^{10,11} It has been considered for piezoelectric properties,¹²⁻¹⁴ and is naturally considered as a wide gap insulator. However, Boonchun and Lambrecht¹⁵ suggested it might be worthwhile considering as a semiconductor electronic material and showed in particular that it could possibly be n-type doped by Ge. That study only used the 16 atom primitive unit cell of LiGaO₂ and thus considered rather high (25 %) Ge_{Ga} doping or Mg_{Li} doping. It did not study the site competition or native defect compensation issues. Here we study the native point defects by means of hybrid functional supercell calculations.

II. COMPUTATIONAL METHOD

Our study is based on density functional calculations using the Heyd-Scuseria-Ernzerhof (HSE) hybrid functional.^{16,17} The calculations are performed using the Vienna Ab-Initio Simulation Package (VASP).^{18,19} The electron ion interactions are described by means of the Projector Augmented Wave (PAW) method.^{20,21} We use a well-converged energy cut-off of 500 eV for the projector augmented plane waves. We performed the calculations with a supercell size of 128 atoms (which corresponds to $2 \times 2 \times 2$ the primitive unit cell) and a single \mathbf{k} -point shifted away from Γ is employed for the Brillouin zone integration. The valence configurations used were $2s^1$ for Li, $3d^{10}4s^24p^1$ for Ga and $2s^22p^4$ for O. In the HSE functional, the Coulomb potential in the exchange energy is divided into short-range and long-range parts with a screening length of 10 Å and only the short-range part of the exact Hartree-Fock non-local exchange is included by mixing it with the generalized gradient Perdew-Burke-Ernzerhof (PBE) potential with a mixing fraction $\alpha = 0.25$. The band gap obtained in this way ($E_g = 5.10$ eV) is still slightly lower than the experimental value.

III. RESULTS

The energy of formation of the defect D^q in charge state q is given by

$$E_f(D^q) = E_{tot}(C : D^q) - E_{tot}(C) - \sum_i \Delta n_i \mu_i + q(\epsilon_v + \epsilon_F + V_{align}) + E_{cor} \quad (1)$$

where $E_{tot}(C : D^q)$ is the total energy of the supercell containing the defect and $E_{tot}(C)$ is the total energy of the perfect crystal supercell. The chemical potentials μ_i represent the energy for adding or removing atoms from the crystal to a reservoir in the process of making the defect. The Δn_i is the change in number of atoms of species

^{a)}Electronic mail: walter.lambrecht@case.edu

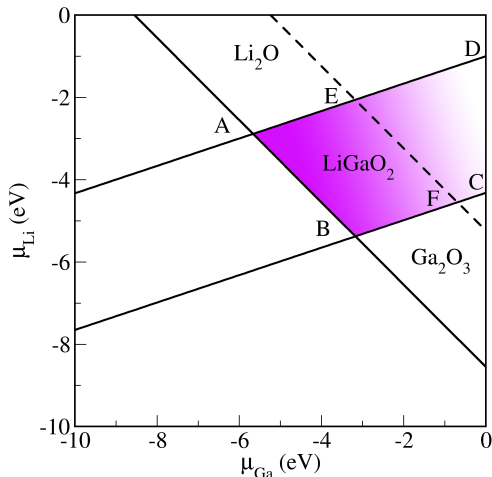


FIG. 1. Chemical potential phase diagram, showing the region of stability of LiGaO_2 . Note that these are excess chemical potentials indicated by $\tilde{\mu}$ in the text.

i. Likewise the chemical potential of the electron determining its charge state is $\epsilon_F + \epsilon_v + V_{align}$ with ϵ_v the energy of an electron at the valence band maximum (VBM) relative to the average electrostatic potential in bulk and ϵ_F the Fermi energy in the gap measured from the VBM. The alignment potential V_{align} represents the alignment of the average electrostatic potential in the supercell far away from the defect relative to that in the bulk. This is calculated using the Freysoldt *et al.* approach.^{22,23} The final term is the image charge correction term which corrects for the Madelung energy of the periodic array of net defect point charges in the uniform background that is added to ensure overall charge neutrality when considering a locally charged defect state. It is closely related to the alignment potential and including these corrections allows one to extrapolate the energy of formation to the dilute limit of an infinitely large supercell.

The chemical potentials $\mu_i = \mu_i^0 + \tilde{\mu}_i$, where μ_i^0 are the chemical potentials of each species in its reference state, namely the phase it occurs in at standard pressure and room temperature, and $\tilde{\mu}_i$ are the excess chemical potentials. The latter are viewed as a tunable parameter reflecting the growth conditions but must obey certain restrictions based on thermodynamic equilibrium. These include

$$\tilde{\mu}_{\text{Li}} + \tilde{\mu}_{\text{Ga}} + 2\tilde{\mu}_{\text{O}} = \tilde{\mu}_{\text{LiGaO}_2} \quad (2)$$

where $\tilde{\mu}_{\text{LiGaO}_2}$ is the energy of formation of LiGaO_2 , which we calculated to be -8.55 eV. Each of the excess chemical potentials $\tilde{\mu}_i \leq 0$ on the left must be less than zero in order to avoid precipitation of the bulk elements Li and Ga or evolving O_2 gas. For example, μ_{Li}^0 corresponds to metallic body-centered-cubic Li and thus $\tilde{\mu}_{\text{Li}} = 0$ corresponds to the assumption that the crystal with the defect is in equilibrium with bulk metallic Li as reservoir. Similarly $\tilde{\mu}_{\text{Ga}} = 0$ corresponds to equilib-

rium with metallic bulk Ga and $\tilde{\mu}_{\text{O}}$ corresponds to O in the O_2 molecule. However, we need to also consider further restrictions imposed by competing binary compounds Ga_2O_3 and Li_2O .

$$\begin{aligned} 2\tilde{\mu}_{\text{Li}} + \tilde{\mu}_{\text{O}} &\leq \tilde{\mu}_{\text{Li}_2\text{O}}, \\ 2\tilde{\mu}_{\text{Ga}} + 3\tilde{\mu}_{\text{O}} &\leq \tilde{\mu}_{\text{Ga}_2\text{O}_3}. \end{aligned} \quad (3)$$

These restrictions determine the region of chemical potentials in which LiGaO_2 is stable relative to the competing binaries and elements. They are bounded by

$$\begin{aligned} \tilde{\mu}_{\text{Li}} &\geq \frac{1}{3}\tilde{\mu}_{\text{Ga}} + [\tilde{\mu}_{\text{LiGaO}_2} - \frac{2}{3}\tilde{\mu}_{\text{Ga}_2\text{O}_3}], \\ \tilde{\mu}_{\text{Li}} &\leq \frac{1}{3}\tilde{\mu}_{\text{Ga}} + \frac{1}{3}[2\tilde{\mu}_{\text{Li}_2\text{O}} - \tilde{\mu}_{\text{LiGaO}_2}]. \end{aligned} \quad (4)$$

with $\tilde{\mu}_{\text{LiGaO}_2} - \frac{2}{3}\tilde{\mu}_{\text{Ga}_2\text{O}_3} = -4.32$ eV and $\frac{1}{3}[2\tilde{\mu}_{\text{Li}_2\text{O}} - \tilde{\mu}_{\text{LiGaO}_2}] = -1.00$ eV.

It is represented in the phase diagram shown in Fig. 1. The points *A, B, C, D* correspond respectively to (A) Li-rich, Ga-poor, (B) Li-poor as well as relative Ga-poor, (C) Ga-rich, Li-poor and (D) Ga-rich and Li-rich but O-poor. The shading of the color is darker the higher the chemical potential of O and the line *AB* corresponds to the O-rich limit $\tilde{\mu}_{\text{O}} = 0$. In addition to the extreme chemical potential conditions (Ga-rich and Li-rich), we consider an intermediate oxygen chemical potential corresponding to a realistic growth condition during the annealing of LiGaO_2 . The oxygen chemical potential is a function of temperature and oxygen partial pressure, as described by Reuter *et al.*²⁴

$$\tilde{\mu}_{\text{O}}(T, p) = \tilde{\mu}_{\text{O}}(T, p_0) + \frac{1}{2}k_B T \ln(p/p_0), \quad (5)$$

where $\tilde{\mu}_{\text{O}}(T, p_0)$ is the oxygen chemical potential at the standard pressure $p_0 = 1$ atm, k_B is Boltzmann's constant, and T is the temperature in Kelvin. In the growth experiment of Ref. 8, the mixed Li_2CO_3 and Ga_2O_3 powders were compressed into tablets and then calcined at 1200 °C for 20 h in air.⁸ We therefore choose an annealing temperature of 1200 °C and an oxygen partial pressure of 0.21 atm which represents the ratio of oxygen gas in ambient environment. The growth conditions at annealing temperature of 1200 °C and oxygen partial pressure of 0.21 atm is represented by the dashed line *EF* in Fig. 1.

The defects considered are the vacancies V_{Ga} , V_{Li} and V_{O} and the antisites Li_{Ga} and Ga_{Li} . The effects of spin polarization were included for cases with unpaired electrons in defect levels. Interstitial defects will be considered in the future but comparison with II-IV-N₂ semiconductors suggest that they would be of high energy.^{25,26} The defect energies of formation are shown for the six chemical potential points *A, B, C, D, E* and *F* in Fig. 2.

First we see that Ga_{Li} is the lowest energy defect for $\epsilon_F = 0$ in all cases. It is a double donor, which is in the $2+$ charge state over most of the gap. Still, it has a well-defined $2+ / 0$ transition making it a negative U system. In Fig. 3 we can see that while for the neutral charge state, the O around Ga_{Li} move outward, they

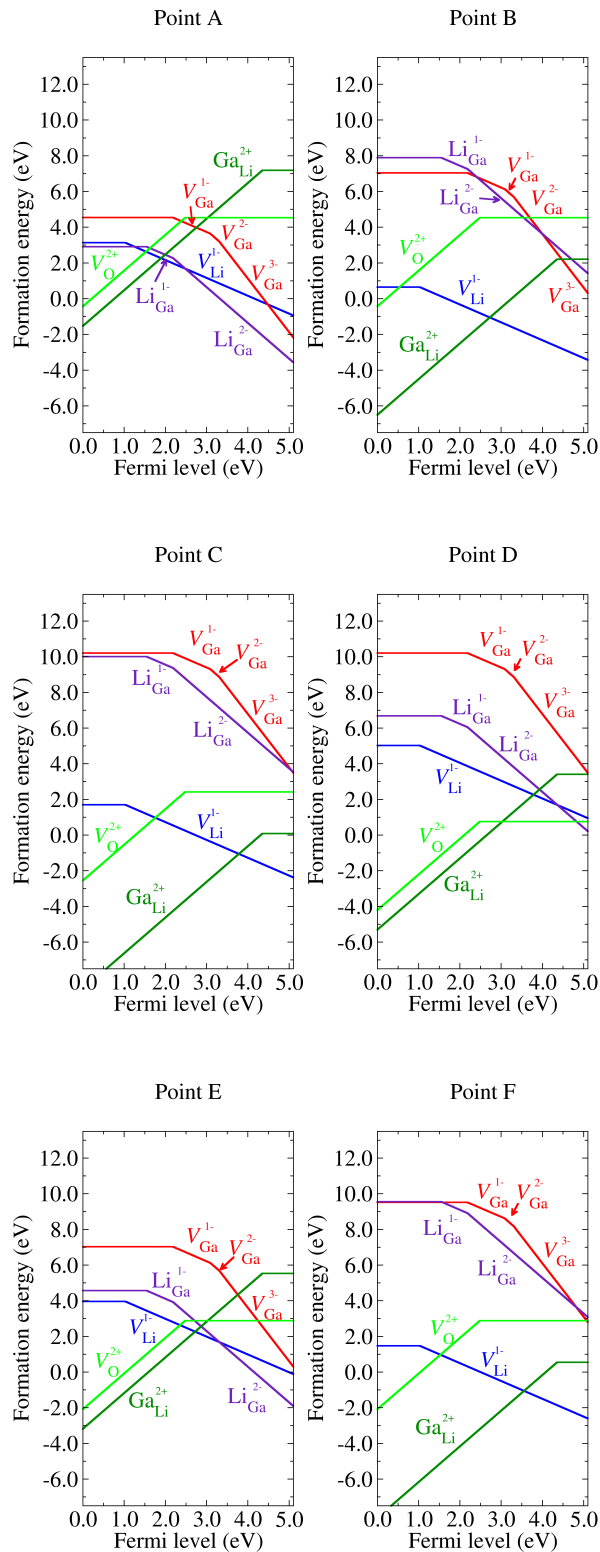


FIG. 2. Energies of formation of various defects in LiGaO_2 for chemical potential conditions identified in Fig. 1.

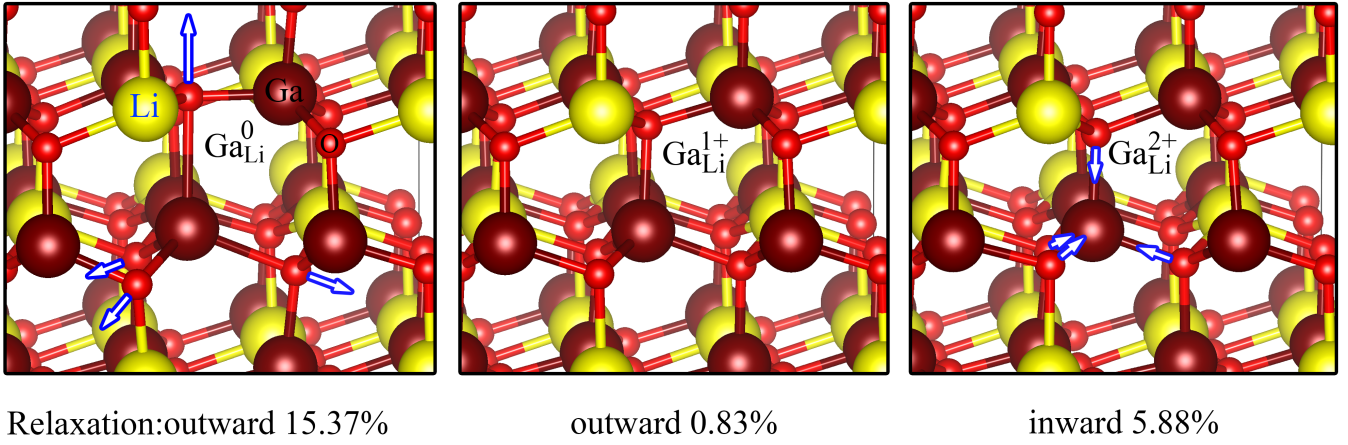
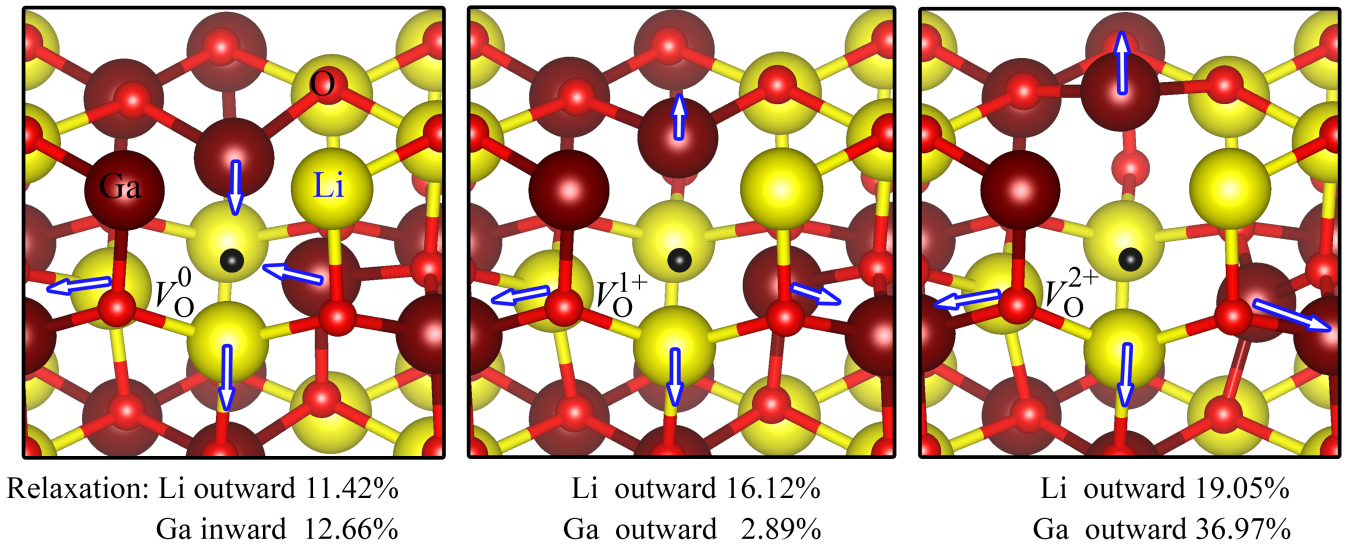
move inward for the 2+ charge state with an in-between outward relaxation for the 1+ state. The additional stabilization by outward motion of the O when adding two electrons rather than one causes the negative U behavior where the 1+ charge state is never the lowest energy one for any Fermi level position. It is thus not behaving like a simple shallow donor, consistent with the relatively deep donor binding energy of 0.74 eV below the conduction band minimum (CBM). We thus do not expect it to be an effective n-type dopant. We can see that this defect has negative energy of formation at $\epsilon_F = 0$ in most cases. This reflects that even in the most Ga-poor case, this defect is hard to avoid because we cannot make the system poor enough in Ga without reaching the stability limit imposed by Li_2O . On the other hand, a Fermi level $\epsilon_F = 0$ is not expected to be realistic as discussed later.

The Li_{Ga} antisite on the other hand is a double acceptor which can occur in 0, -1, -2 charge states. It is the lowest energy defect in its 2- charge state near the CBM in cases A, D and E. These are the cases richest in Li.

As for the vacancies, V_{Li} occurs in 0, -1 charge states, while V_{Ga} occurs in 0, -1, -2, -3 charge states. We can see that V_{Ga}^0 has a high energy of formation in all cases. Although its negative charge states have significantly lower energy for ϵ_F close to the CBM, it never becomes the lowest energy defect and therefore does not play a role in determining the Fermi level. The V_{Li} is more interesting. Although it has high energy in the Li-rich case D (which is somewhat unrealistic and O-poor) it has low energy in the Li-poor cases, B, C, F. Even in case E, its intersection with the $\text{Ga}_{\text{Li}}^{2+}$ occurs close to that of the intersection of the latter with $\text{Li}_{\text{Ga}}^{2-}$. We thus expect that both these acceptors may play a role in compensating the $\text{Ga}_{\text{Li}}^{2+}$.

Turning now to the O-vacancies, there are two non-equivalent sites for the oxygen in LiGaO_2 : on top of Li (O_1) or on top of Ga (O_2). We find that both $V_{\text{O}1}$ and $V_{\text{O}2}$ are only stable in the neutral and 2+ charge states (with $V_{\text{O}2}$ slightly lower in energy than $V_{\text{O}1}$) with the transition level (2+/0) at 2.48 eV above the VBM or 2.62 eV below the CBM. This is a quite deep donor level and indicates that the vacancy is also a negative U center. In Fig. 4 one can see that also in this case the relaxations are strongly charge-state dependent. This figure shows the relaxations near a $V_{\text{O}2}$ but similar results hold for $V_{\text{O}1}$. In the neutral charge state, the Ga move inward, while the Li move outward. In the 2+ state both move strongly outward. This is similar to the V_{O} in ZnO ^{15,27} although the level is here even deeper and close to mid gap. We find that the V_{O}^{2+} energy of formation is negative for Fermi levels close to the VBM for points C, D, E, F. They become positive for the O-rich limits (A, B). Its energy of formation is always higher than that of the $\text{Ga}_{\text{Li}}^{2+}$ and thus it is not expected to play a significant role in the charge balance.

Using the charge neutrality condition between free electron concentration $n_e(T, \epsilon_F)$, free hole concentration

FIG. 3. Structural relaxation for Ga_{Li} in different charge states.FIG. 4. Structural relaxation for V_{O_2} in different charge states.

$n_h(T, \epsilon_F)$ and the various defect concentrations,

$$c(D^q; T, \epsilon_F) = N_D g(q) e^{-(E_f(D^q, \epsilon_F=0) + q\epsilon_F)/k_B T} \quad (6)$$

where N_D is the number of available sites per cm^3 and $g(q)$ a degeneracy factor depending on the charge state, we can find the equilibrium Fermi level and the defect concentrations for a given temperature following the procedure of Ref.25. For the electron and hole concentrations we use a parabolic band with effective density of states masses $m_e^* \approx 0.4$ and $m_h^* \approx 1.8$ (as obtained from the calculate hybrid functional band structure and averaging over directions.) For a temperature of $T = 1500$ K close to the growth temperature, we find that under chemical potential conditions C , the equilibrium Fermi level is $\epsilon_F = 3.815$ eV, close to the intersection of the

$\text{V}_{\text{Li}}^{1-}$ and $\text{Ga}_{\text{Li}}^{2+}$. The electron concentration $n_e = 6 \times 10^{13} \text{ cm}^{-3}$ but the $[\text{V}_{\text{Li}}^{-1}] = 2[\text{Ga}_{\text{Li}}^{2+}] = 1.0 \times 10^{26} \text{ cm}^{-3}$ are unrealistically high. This is related to the energies of formation of the main defects Ga_{Li} and V_{Li} being negative for the equilibrium Fermi level. For point E , the equilibrium Fermi level position is closer to mid gap, $\epsilon_F = 2.75$ eV with $[\text{Ga}_{\text{Li}}^{2+}] = 3.7 \times 10^{14}$, $[\text{V}_{\text{Li}}^{-1}] = 7.22 \times 10^{14}$ and $[\text{Li}_{\text{Ga}}^{2-}] = 1 \times 10^{13} \text{ cm}^{-3}$, $[\text{V}_{\text{O}}^{2+}] = 5 \times 10^{12} \text{ cm}^{-3}$. So, in this case the concentrations of defects are much smaller and the $\text{Ga}_{\text{Li}}^{2+}$ is still mostly compensated by $\text{V}_{\text{Li}}^{-1}$ but partially also by $\text{Li}_{\text{Ga}}^{2-}$. The electron concentration at $n_e = 3.2 \times 10^{12} \text{ cm}^{-3}$ is then only slightly higher than the hole concentration $n_h = 1.6 \times 10^{11} \text{ cm}^{-3}$ but both free carrier concentrations are in fact negligible under both chemical potential conditions considered. Even un-

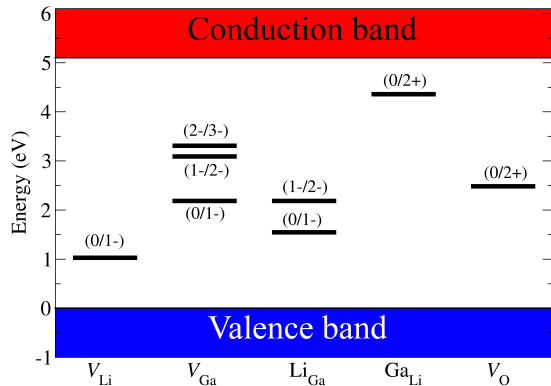


FIG. 5. Defect transition levels in LiGaO₂.

der the most Ga-poor conditions (point A), Ga_{Li}²⁺ is the dominant defect and is compensated mostly by V_{Li}¹⁻. In this case, $\epsilon_F = 1.92$ eV is closest to the VBM and the material would then be slightly *p*-type with $n_h = 9.7 \times 10^{13}$ cm⁻³.

TABLE I. Transition levels $\epsilon(q, q')$ in eV relative to the VBM

Defect	q, q'	$\epsilon(q, q')$
V _{Li}	(0/1-)	1.0270
V _{Ga}	(0/1-)	2.1843
	(1-/2-)	3.0899
	(2-/3-)	3.3088
Li _{Ga}	(0/1-)	1.5464
	(1-/2-)	2.1855
Ga _{Li}	(0/2+)	4.3569
V _O	(0/2+)	2.4831

It is instructive to compare the defect physics in this system to that in II-IV-N₂ semiconductors like ZnGeN₂,²⁵. The similarity is that in both cases, the antisites play a crucial role. However, the dependence on chemical potentials of the elements is more important here because a wider region of stability occurs. Furthermore the Ga_{Li} antisite is here not a shallow but a deep donor and is thus not expected to lead to unintentional n-type doping. This is consistent with the insulating behavior of LiGaO₂. However, it does not exclude the possibility of n-type doping by Si or Ge or Sn which will be studied separately.

The main defect transition levels in the gap are summarized in Table I and in Fig. 5.

IV. CONCLUSIONS

In this paper we have studied the native defects in LiGaO₂. We find that the relative energy of formation of vacancies and antisites depends strongly on the chemical potential conditions. The Ga_{Li} antisite is a dominant donor defect. However, it has a rather deep 2 + /0 donor

level and is a negative *U* center. It is thus not expected to lead to significant n-type doping. It furthermore becomes compensated mostly by V_{Li}¹⁻ and in part by Li_{Ga}²⁻ depending on how rich the system is in Li. The V_O is found to be an even deeper double donor negative *U* center. The defect transition levels are all relatively deep in to the gap with no truly shallow levels.

ACKNOWLEDGMENTS

The work at CWRU was supported by the U.S. National Science Foundation under grant No. 1755479. The work at Kasetsart was supported by Kasetsart University Research and Development Institute (KURDI).

- ¹K. Sasaki, M. Higashiwaki, A. Kuramata, T. Masui, and S. Yamakoshi, “[MBE] grown ga2o3 and its power device applications”, J. Cryst. Growth **378**, 591 – 595 (2013), the 17th International Conference on Molecular Beam Epitaxy.
- ²A. J. Green, K. D. Chabak, E. R. Heller, R. C. Fitch, M. Baldini, A. Fiedler, K. Irmscher, G. Wagner, Z. Galazka, S. E. Tetlak, A. Crespo, K. Leedy, and G. H. Jessen, “3.8-MV/cm Breakdown Strength of MOVPE-Grown Sn-Doped β -Ga2O3 MOSFETs,” IEEE Electron Device Letters **37**, 902–905 (2016).
- ³M. Marezio, “The crystal structure of LiGaO₂,” Acta Crystallographica **18**, 481–484 (1965).
- ⁴T. Ishii, Y. Tazoh, and S. Miyazawa, “Single-crystal growth of LiGaO₂ for a substrate of GaN thin films,” J. Crystal Growth **186**, 409 – 419 (1998).
- ⁵J. T. Wolan and G. B. Hoflund, “Chemical alteration of the native oxide layer on ligao2(001) by exposure to hyperthermal atomic hydrogen,” J. Vac. Sci. Tech. A **16**, 3414–3419 (1998).
- ⁶N. W. Johnson, J. A. McLeod, and A. Moewes, “The electronic structure of lithium metagallate,” Journal of Physics: Condensed Matter **23**, 445501 (2011).
- ⁷I. Ohkubo, C. Hirose, K. Tamura, J. Nishii, H. Saito, H. Koinuma, P. Ahemt, T. Chikyow, T. Ishii, S. Miyazawa, Y. Segawa, T. Fukumura, and M. Kawasaki, “Heteroepitaxial growth of -ligao2 thin films on zno,” Journal of Applied Physics **92**, 5587–5589 (2002).
- ⁸C. Chen, C.-A. Li, S.-H. Yu, and M. M. Chou, “Growth and characterization of β -LiGaO₂ single crystal,” Journal of Crystal Growth **402**, 325 – 329 (2014).
- ⁹A. Boonchun and W. R. L. Lambrecht, “Electronic structure, doping, and lattice dynamics of LiGaO₂,” in *Oxide-based Materials and Devices II*, Proceedings of SPIE, Vol. 7940, edited by F. H. Terani, D. C. Look, and D. J. Rogers (2011) p. 79400N.
- ¹⁰T. Omata, K. Tanaka, A. Tazuke, K. Nose, and S. Otsuka-Yao-Matsuo, “Wide band gap semiconductor alloy: x(LiGaO₂)12(1-x)ZnO,” J. Appl. Phys. **103**, 083706 (2008).
- ¹¹T. Omata, M. Kita, K. Nose, K. Tachibana, and S. Otsuka-Yao-Matsuo, “Zn2LiGaO4, Wurtzite-Derived Wide Band Gap Oxide,” Jpn. J. Appl. Phys. **50**, 031102 (2011).
- ¹²S. Nanamatsu, K. Doi, and M. Takahashi, “Piezoelectric, elastic and dielectric properties of LiGaO₂,” Japanese Journal of Applied Physics **11**, 816–822 (1972).
- ¹³S. N. Gupta, J. F. Vetelino, V. B. Jipson, and J. C. Field, “Surface acoustic wave properties of lithium gallium oxide,” Journal of Applied Physics **47**, 858–860 (1976).
- ¹⁴A. Boonchun and W. R. L. Lambrecht, “First-principles study of the elasticity, piezoelectricity, and vibrational modes in ligao2 compared with zno and gan,” Phys. Rev. B **81**, 235214 (2010).
- ¹⁵A. Boonchun and W. R. L. Lambrecht, “Critical evaluation of the LDARU approach for band gap corrections in point defect calculations: The oxygen vacancy in ZnO case study,” Phys. Stat. Solidi (b) **248**, 1043–1051 (2011).

- ¹⁶J. Heyd, G. E. Scuseria, and M. Ernzerhof, “Hybrid functionals based on a screened coulomb potential,” *J. Chem. Phys.* **118**, 8207–8215 (2003).
- ¹⁷J. Heyd, G. E. Scuseria, and M. Ernzerhof, “Erratum: “hybrid functionals based on a screened coulomb potential” [j. chem. phys. [bold 118], 8207 (2003)],” *J. Chem. Phys.* **124**, 219906 (2006).
- ¹⁸<https://www.vasp.at/>.
- ¹⁹G. Kresse and J. Furthmüller, “Efficiency of ab-initio total energy calculations for metals and semiconductors using a plane-wave basis set,” *Computational Materials Science* **6**, 15–50 (1996).
- ²⁰P. E. Blöchl, “Projector augmented-wave method,” *Phys. Rev. B* **50**, 17953–17979 (1994).
- ²¹G. Kresse and D. Joubert, “From ultrasoft pseudopotentials to the projector augmented-wave method,” *Phys. Rev. B* **59**, 1758–1775 (1999).
- ²²C. Freysoldt, J. Neugebauer, and C. G. Van de Walle, “Fully *Ab Initio* finite-size corrections for charged-defect supercell calculations,” *Phys. Rev. Lett.* **102**, 016402 (2009).
- ²³C. Freysoldt, B. Grabowski, T. Hickel, J. Neugebauer, G. Kresse, A. Janotti, and C. G. Van de Walle, “First-principles calculations for point defects in solids,” *Rev. Mod. Phys.* **86**, 253–305 (2014).
- ²⁴K. Reuter and M. Scheffler, “Composition, structure, and stability of RuO₂(110) as a function of oxygen pressure,” *Phys. Rev. B* **65**, 035406 (2001).
- ²⁵D. Skachkov, A. Punya Jaroenjittichai, L.-y. Huang, and W. R. L. Lambrecht, “Native point defects and doping in ZnGeN₂,” *Phys. Rev. B* **93**, 155202 (2016).
- ²⁶D. Skachkov and W. R. L. Lambrecht, “Native interstitial defects in ZnGeN₂,” *Phys. Rev. Materials* **1**, 054604 (2017).
- ²⁷A. Boonchun and W. R. L. Lambrecht, “Electronic structure of defects and doping in ZnO: Oxygen vacancy and nitrogen doping,” *Phys. Stat. Solidi (b)* **250**, 2091–2101 (2013).